British Journal of Pharmacology (2000) 131, 729–739

www.nature.com/bjp

Identification of a novel nicotinic binding site in mouse brain using [^{125}I]-epibatidine

*,[1]Paul Whiteaker, [1]Melissa Jimenez, [2,3]J. Michael McIntosh, [1]Allan C. Collins & [1]Michael J. Marks

[1]Institute for Behavioral Genetics, University of Colorado, Boulder, Colorado, CO 80303 U.S.A.; [2]Department of Biology, University of Utah, Salt Lake City, Utah, UT 84112, U.S.A. and [3]Department of Psychiatry, University of Utah, Salt Lake City, Utah, UT 84112, U.S.A.

1 [^{125}I]-Epibatidine binds to multiple nicotinic acetylcholine receptor (nAChR) subtypes with high affinity. In this study, [^{125}I]-epibatidine was used to label and characterize a novel nAChR subtype found in mouse brain inferior colliculus, interpeduncular nucleus, and olfactory bulb homogenates.

2 Binding of [^{125}I]-epibatidine was saturable and apparently monophasic in each brain region ($K_D = 71 \pm 12$ pM mean $\pm$ s.e.mean across regions) but inhibition of [^{125}I]-epibatidine binding (200 pM) by A85380, cytisine and (−)-nicotine was biphasic, indicating the presence of multiple binding sites.

3 The sites with lower agonist affinity comprised 30.0 ± 2.2, 58.6 ± 0.1 and 48.7 ± 3.3% of specific [^{125}I]-epibatidine (200 pM) binding in inferior colliculus, interpeduncular nucleus, and olfactory bulb homogenates, respectively.

4 The affinity difference between A85380-sensitive and -resistant binding sites was particularly marked (approximately 1000 fold). Thus A85380 was used to differentiate agonist-sensitive and -resistant sites.

5 The pharmacological profiles of the A85380-resistant sites in each region were assessed with inhibition binding experiments, using 14 agonists and five antagonists. The profiles were indistinguishable across regions, implying that A85380-resistant [^{125}I]-epibatidine binding sites in inferior colliculus, interpeduncular nucleus, and olfactory bulb represent a single nAChR subtype.

6 The pharmacological profile of the A85380-resistant sites is very different from that previously reported for high affinity (−)-[^{3}H]-nicotine-, [^{125}I]-α-bungarotoxin-, or [^{125}I]-α-conotoxin MII-binding sites, suggesting that they represent a novel nAChR population in mouse brain.

British Journal of Pharmacology (2000) **131,** 729–739

Keywords: Nicotinic acetylcholine receptor; neuronal; mouse brain; [^{125}I]-epibatidine

Abbreviations: α-CtxMII, α-conotoxin MII; A85380, 3-(2(S)-Azetidinylmethoxy)pyridine dihydrochloride; CNS, central nervous system; DHβE, dihydro-β-erythroidine; HEPES, 4-(2-hydroxyethyl)-1-piperazineethanesulphonic acid; MCC, methylcarbamycholine; mRNA, messenger RNA; nAChR, nicotinic acetylcholine receptor; PEI, polyethyleneimine

Introduction

Interest in and research into the properties and function of centrally expressed neuronal nicotinic acetylcholine receptors (nAChRs) has increased steadily over the last decade, partially driven by the realization that nAChRs are physiologically relevant in a wide range of CNS functions (such as analgesia, cognition, motor control, and reward), and may be involved in pathological states such as Alzheimer's and Parkinson's diseases and Tourette's syndrome (Dani & Heinemann, 1996; Decker & Arneric, 1998). To date, molecular cloning has identified nine nAChR subunits (α_{2-7}, β_{2-4}) expressed in varying patterns and quantities throughout the mammalian brain. Since mature nAChRs appear to be pentameric assemblies of these subunits, and differing subunit compositions produce different nAChR subtypes, the potential nAChR subtype diversity is vast (Lindstrom *et al*., 1996).

Identifying individual nAChR subtypes in the CNS has been a difficult undertaking. The 'high affinity agonist binding' $\alpha_4\beta_2$ subtype (labelled by [^{3}H]-acetylcholine, [^{3}H]-cytisine, [^{3}H]-methylcarbamylcholine and (−)-[^{3}H]-nicotine; Whiting & Lindstrom, 1987; Flores *et al*., 1992; Picciotto *et al*., 1995; Marubio *et al*., 1999) and the predominantly or entirely α_7 subtype (labelled by [^{125}I]-α-Bgt, Schoepfer *et al*., 1990; Seguela *et al*., 1992; Orr-Urtreger *et al*., 1997) have been extensively characterized, but information on other central nervous system nAChR subtypes is sketchy at best. A lack of labelled ligands that bind these other subtypes, and a paucity of subtype selective pharmacological tools has hampered the study of neuronal nAChR subtypes. Nevertheless, this search remains a priority for a number of reasons: (1) knowledge of which native subtypes are expressed will yield insights into the rules governing assembly of subunit peptides into receptor proteins; (2) once additional subtypes are positively identified, it will become easier to isolate or generate subtype specific compounds; and (3) determining the physiological roles of individual neuronal nAChR subtypes in normal and/or pathological states will allow the development of better targeted nicotinic therapies.

The discovery that [^{3}H]-epibatidine binds to multiple nAChR subtypes with high affinity (Houghtling *et al*., 1995; Perry & Kellar, 1995; Flores *et al*., 1996; Marks *et al*., 1998; Parker *et al*., 1998) provided a tool to identify novel nAChR subtypes. In rat (Houghtling *et al*., 1995) and mouse (Marks *et al*., 1998) CNS, the majority of high affinity [^{3}H]-epibatidine binding occurs at the $\alpha_4\beta_2$ subtype nAChR, but additional sites (distinguished by their relatively low cytisine affinity) are also expressed in small

*Author for correspondence at: Institute for Behavioral Genetics, University of Colorado, Campus Box 447, Boulder, CO 80303-0447, U.S.A.

nuclei, dispersed across the brain. More recently, Whiteaker *et al*. (2000b) have subdivided these cytisine-resistant [^{3}H]-epibatidine binding sites into two groups: those with high (nanomolar) affinity for the $\alpha_3\beta_2$-selective ligand α-conotoxin MII (α-CtxMII; Cartier *et al*., 1996), and those with lower affinity for α-CtxMII. Although this approach has been informative, a thorough examination of the cytisine-resistant sites' properties has been impractical, due to a combination of their scarcity (approximately 15% of the mouse brain [^{3}H]-epibatidine binding population is cytisine-resistant), and [^{3}H]-epibatidine's low specific activity (30–50 Ci mmol^{-1}). Fortunately, a higher specific activity, ^{125}I-labelled version of epibatidine ([^{125}I]-epibatidine) is now available. Studies in mammalian brain homogenates and brain slices (Davila-Garcia *et al*., 1997), indicated that this ligand retains the favourable properties of [^{3}H]-epibatidine (high affinity, low non-specific binding, labelling of multiple nAChR subtypes), while providing increased specific activity (2200 Ci mmol^{-1}) and increased detection efficiency ($\approx$80–85% for ^{125}I *vs* $\approx$40–45% for ^{3}H). Theoretically, this combination should boost signals by approximately 100 fold, making investigations of rarer nAChR subtypes practical.

In this study, [^{125}I]-epibatidine was used to characterize the cytisine- and α-CtxMII-resistant population of epibatidine binding nAChRs, found predominantly in the inferior colliculus, medial habenula-interpeduncular nucleus tract and olfactory bulbs (Whiteaker *et al*., 2000b). The pharmacology and distribution of these sites was indistinguishable across the three brain regions, and different from that of previously characterized nAChR subtypes, suggesting that they represent a novel nAChR population in mouse brain. The success of this approach suggests that the use of [^{125}I]-epibatidine, in conjunction with selective pharmacology, will provide a widely applicable method for identifying and characterizing novel, native nAChR subtypes.

Methods

Animals

Male mice (C57BL/6J, 60–90 days old) were used throughout this study. Mice were bred at the Institute for Behavioral Genetics and housed five per cage. The vivarium was maintained on a 12 h light/dark cycle (lights on 0700 to 1900 h), and mice were given free access to food and water. All procedures used in this study were approved by the Animal Care and Utilization Committee of the University of Colorado, Boulder (CO, U.S.A.)

Materials

Uridine triphosphate (α-^{35}S, initial specific activity = 800 Ci mmol^{-1}), [^{3}H]-epibatidine (specific activity = 33.8 Ci mmol^{-1}), and [^{125}I]-epibatidine (specific activity = 2200 Ci mmol^{-1}) were obtained from DuPont NEN (Boston, MA, U.S.A.). (−)-Nicotine bitartrate was bought from BDH Chemicals (Poole, U.K.). 3-(2(S)-Azetidinylmethoxy)pyridine dihydrochloride (A85380), dihydro-β-erythroidine hydrobromide, epibatidine dihydrochloride (DHβE), epiboxidine hydrochloride, and methylcarbamylcholine chloride (MCC) were ordered from RBI (Nantick, MA, U.S.A.). α-CtxMII was synthesized as described previously (Cartier *et al*., 1996). Microscope slides were bought from Richard Allen, Richland, MI, U.S.A. All other supplies were purchased from Sigma Chemical Co. (St. Louis, MO, U.S.A.).

Membrane preparation

Each C57BL/6J mouse was killed by cervical dislocation. The brain was removed from the skull and placed on an ice-cold platform. Tissue was collected from inferior colliculus, interpeduncular nucleus, and olfactory bulbs, then homogenized in ice-cold hypotonic buffer (mM: NaCl, 14.4; KCl, 0.2; $CaCl_2$, 0.2; $MgSO_4$, 0.1; HEPES 2; pH = 7.5) using a glass-Teflon tissue grinder (Marks *et al*., 1998). Particulate fractions were obtained by centrifugation at 20,000 × *g* (15 min, 4°C; Sorval RC-2B centrifuge). The pellets were resuspended in fresh homogenization buffer, incubated at 22°C for 10 min, then harvested by centrifugation as before. Each pellet was washed twice more by resuspension/centrifugation, then stored (in pellet form under homogenization buffer) at −70°C until used. Protein was quantified according to the method of Lowry *et al*. (1951), using bovine serum albumin as the standard.

[^{125}I]-Epibatidine saturation binding to membranes

Binding of [^{125}I]-epibatidine was quantified using a modified version of the methods previously described for [^{3}H]-epibatidine (Marks *et al*., 1998). Incubations were performed in 96-well polystyrene plates, in 30 μl of binding buffer (mM: NaCl, 144; KCl, 1.5; $CaCl_2$, 2; $MgSO_4$, 1; HEPES, 20; pH = 7.5). Plates were covered to minimize evaporation during incubation, and all incubations progressed for 2 h at 22°C. Saturation binding experiments were performed for membrane preparations from each brain region, using ligand concentrations ranging between approximately 4–500 pM. Binding reactions were terminated by filtration of samples onto a single thickness of polyethyleneimine-soaked (0.5% w v^{-1} in binding buffer) GFA/E glass fibre filters (Gelman Sciences, Ann Arbor, MI, U.S.A.) using an Inotech Cell Harvester (Inotech, Rockville, MD, U.S.A.). Samples were subsequently washed six times with ice-cold binding buffer. Total and non-specific (in the presence of 1 mM (−)-nicotine tartrate) binding were determined in duplicate for each [^{125}I]-epibatidine concentration. Bound ligand was quantified by gamma counting at 83–85% efficiency, using a Packard Cobra counter. At the lower concentrations, a significant proportion (up to 20%) of ligand bound to the tissue. Free [^{125}I]-epibatidine concentrations were estimated by correcting for the amount of ligand bound to tissue, and these corrected concentrations were used to calculate K_D values for [^{125}I]-epibatidine binding in each brain region.

[^{125}I]-Epibatidine inhibition binding to membranes

Inhibition binding experiments were performed using 200 pM [^{125}I]-epibatidine (equivalent to 500 Bq well^{-1}). The amount of membrane protein added was chosen to produce maximum binding of ligand to the tissue of approximately 40 Bq well^{-1} (less than 10% of total ligand added, minimizing the effects of ligand depletion). Where peptide ligands were used, the medium was supplemented with bovine serum albumin (0.1% w v^{-1}) as a carrier protein. Various concentrations of competing drugs were included in duplicate wells. When A85380-resistant [^{125}I]-epibatidine binding populations were investigated, 10 nM A85380 was incorporated into the whole assay by addition to the [^{125}I]-epibatidine solution. Non-specific binding was determined in the presence of 1 mM (−)-nicotine tartrate for each experiment.

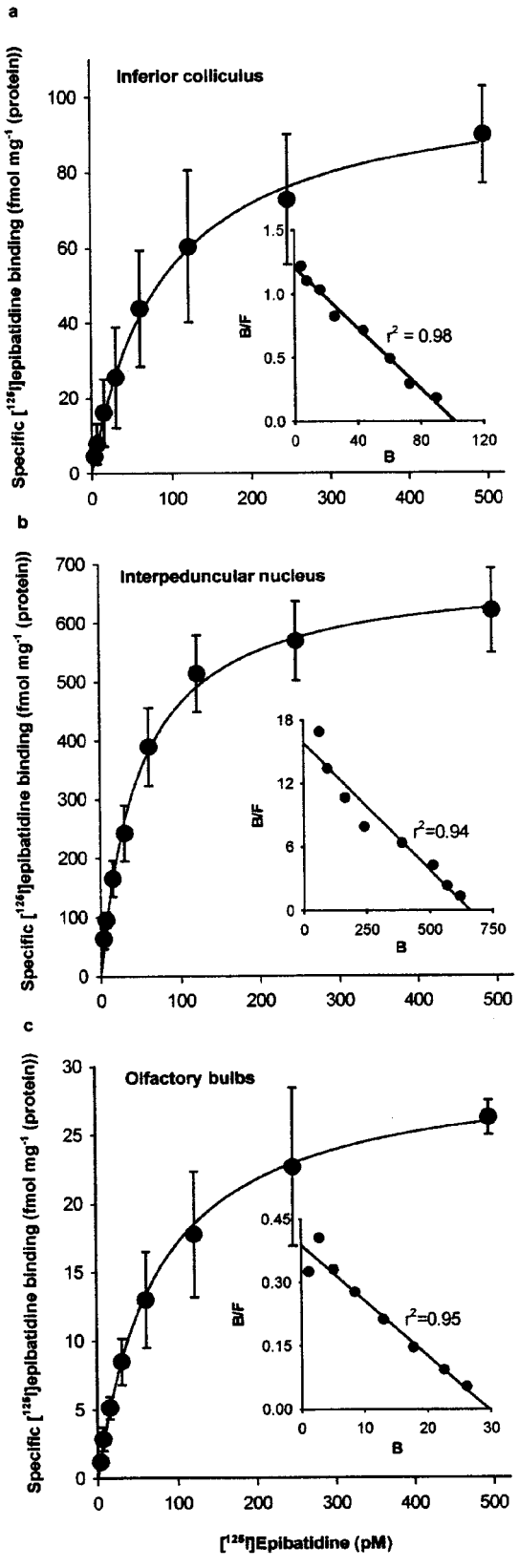

Figure 1 Saturation binding of [^{125}I]-epibatidine to inferior colliculus, interpeduncular nucleus, and olfactory bulb membranes. Particulate fractions from mouse brain regions (a, inferior colliculus; b, interpeduncular nucleus; c, olfactory bulbs) were incubated at 22°C with [^{125}I]-epibatidine (4–500 pM; see Methods). Non-specific binding was determined by addition of (−)-nicotine (1 mM), and represented less than 2% of specific binding even at the highest ligand concentration used. Specific binding was calculated as the difference between total and non-specific binding for each experiment, and fitted to a single site Hill equation (see Methods). The data in each region were subjected to Scatchard analysis (inset panels), and showed no evidence for multiple [^{125}I]-epibatidine binding sites. Each point represents the mean±s.e.mean of three separate determinations.

Simultaneous determination of A85380-sensitive and -resistant [^{125}I]-epibatidine saturation binding to membranes

As for [^{125}I]-epibatidine saturation binding, experiments were performed for membrane preparations from each brain region, using the same assay volumes and incubation times, and ligand concentrations in the range of approximately 4–500 pM. At each concentration of [^{125}I]-epibatidine, the ability of A85380 to inhibit specific [^{125}I]-epibatidine binding was determined at a range of A85380 concentrations. This allowed the amount of specific A85380-sensitive and -resistant [^{125}I]-epibatidine binding at each [^{125}I]-epibatidine concentration to be quantified. Independent saturation analyses were then performed for the two populations.

Autoradiography, [^{3}H]-epibatidine binding and mRNA in situ *hybridization*

C57BL/6J mice were killed by cervical dislocation, the brains were removed from the skull and rapidly frozen by immersion in isopentane (−35°C, 10 s). The frozen brains were wrapped in aluminium foil, packed in ice, and stored at −70°C until sectioning. Tissue sections (14 μm thick) prepared using an IEC Minotome Cryostat refrigerated to −16°C were thaw mounted onto subbed microscope slides (Simmons *et al.*, 1989). Mounted sections were stored, desiccated, at −70°C until use. Between six and 10 series of sections were made from each mouse.

[^{3}H]-Epibatidine autoradiography procedures were similar to those described previously (Pauly *et al.*, 1989; Marks *et al.*, 1998; Whiteaker *et al.*, 2000b). Sections for use in [^{3}H]-epibatidine binding were incubated in binding buffer (mM: NaCl, 144; KCl, 1.5; $CaCl_2$, 2; $MgSO_4$, 1; HEPES, 20; bovine serum albumin, 0.1% (w v^{-1}); pH = 7.5) at 22°C for 15 min, followed by incubation with 500 pM [^{3}H]-epibatidine for 2 h at 22°C. On the basis of results obtained by Whiteaker *et al.* (2000b), cytisine-resistant [^{3}H]-epibatidine binding was measured in the presence of 100 nM cytisine, while cytisine- and α-CtxMII-resistant [^{3}H]-epibatidine binding was defined using 100 nM cytisine + 20 nM α-CtxMII. Non-specific [^{3}H]-epibatidine binding (in the presence of 1 mM (−)-nicotine) was indistinguishable from film background. Slides were washed by sequential incubation in the following buffers (all steps at 0°C): 5 s in binding buffer (twice), 5 s in 0.1 × binding buffer (twice), and twice for 5 s in 5 mM HEPES (pH = 7.5). Sections were initially dried with a stream of air, then by overnight storage (22°C) under vacuum. Mounted, desiccated sections were apposed to Amersham Hyperfilm-^{3}H for 8 weeks before development. Digital image collection was performed by illuminating films using a Northern Light light box, and autoradiographic images of the sections were captured using a CCD imager camera.

The method used for *in situ* hybridization using riboprobes was identical to that used by Simmons *et al.* (1989), Marks *et al.* (1992), and Whiteaker *et al.* (2000b). Probes were prepared by *in vitro* transcription, using α-^{35}S-UTP as the sole source of UTP. Synthesis was designed to yield full-length antisense transcript. Immediately before hybridization, the probe was subjected to alkaline hydrolysis using the method of Cox *et al.* (1984) to yield products with average sizes of 500 bases.

Following hybridization, slides were air-dried and stored under vacuum overnight before exposure to Amersham Hyperfilm β-Max film (10–20 days). Autoradiographic images were captured as described above for [^{3}H]-epibatidine binding.

Calculations

Results for saturation binding experiments were calculated using the Hill equation: $B = B_{max}\ L^n/(L^n + K_D{}^n)$ where B is the binding at the free ligand concentration L, B_{max} is the maximum number of binding sites, K_D is the equilibrium binding constant, and n is the Hill coefficient. Values of B_{max}, K_D, and n were calculated using the non-linear least squares fitting algorithm of SigmaPlot V5.0 (Jandel Scientific, San Rafael, CA, U.S.A.). Results for inhibition of [^{125}I]-epibatidine binding were calculated using either a one-site fit: $B = B_o/(1 + (I/IC_{50}))$ where B is ligand bound at inhibitor concentration I, B_o is the binding in the absence of inhibitor, and IC_{50} is the concentration of inhibitor required to reduce binding to 50% of B_o, or a two site fit: $B = B_1/(1 + (I/IC_{50\text{-}1})) + B_2/(1 + (1/IC_{50\text{-}2}))$ where B is ligand bound at inhibitor concentration I, and B_1 and B_2 are binding sites sensitive to inhibition with $IC_{50\text{-}1}$ and $IC_{50\text{-}2}$, respectively. Values for K_i (inhibition binding constant) were derived by the method of Cheng & Prusoff (1973): $K_i = IC_{50}/1 + (L/K_D)$.

Results

[^{125}I]-Epibatidine saturation and cytisine-resistant binding in inferior colliculus, interpeduncular nucleus, and olfactory bulbs

The mouse brain regions (inferior colliculus, interpeduncular nucleus, and olfactory bulbs) used in this investigation were

Table 1 [^{125}I]-epibatidine saturation binding in inferior colliculus, interpeduncular nucleus, and olfactory bulbs

Region	B_{max} (fmol mg^{-1} (protein))	K_D (pM)	n_H
Inferior colliculus	103.6±2.7	89.2±6.6	0.96±0.08
Interpeduncular nucleus	687.3±86.7	48.6±11.8	1.01±0.09
Olfactory bulbs	29.9±8.5	74.8±5.9	0.99±0.06

Specific binding of [^{125}I]-epibatidine was determined for differing ligand concentrations (4–500 pM), as described in the Methods section. Values of B_{max} and K_D were calculated for each individual experiment using the Hill equation. Each value presented is the mean±s.e.mean of three individual determinations.

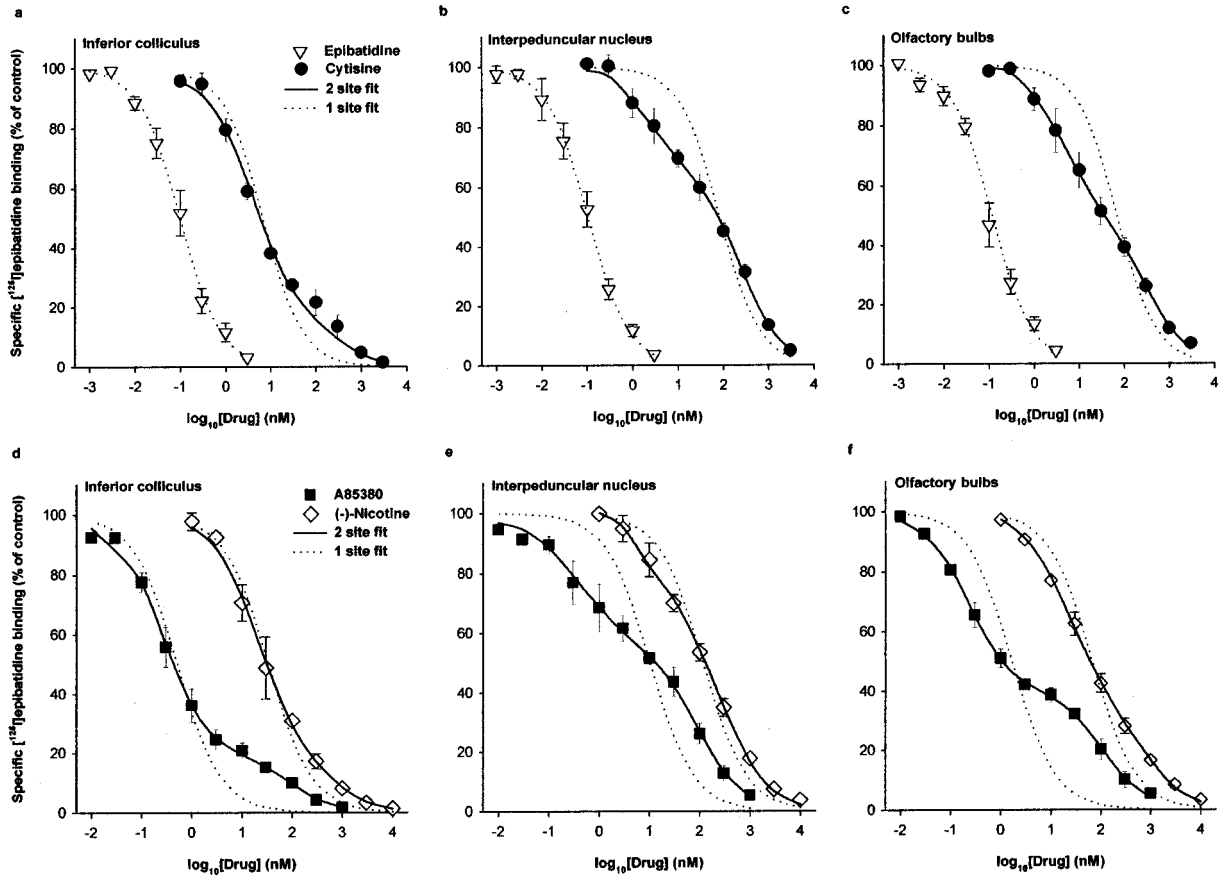

Figure 2 Competition by cytisine, epibatidine, A85380, and (−)-nicotine for [^{125}I]-epibatidine binding sites in regionally dissected mouse brain membranes. Top row: mouse brain particulate fractions prepared from (a) inferior colliculus, (b) interpeduncular nucleus, and (c) olfactory bulbs were incubated at 22°C with [^{125}I]-epibatidine (200 pM, 2 h) in the presence of cytisine (0.3 nM–3 μM) or epibatidine (1 pM–3 nM). Bottom row: (d) inferior colliculus, (e) interpeduncular nucleus, and (f) olfactory bulb particulate fractions were incubated at 22°C with [^{125}I]-epibatidine (200 pM, 2 h) in the presence of A85380 (10 pM–1 μM) or (−)-nicotine (1 nM–10 μM). In all cases non-specific binding was determined in the presence of 1 mM (−)-nicotine. Each point represents the mean±s.e.mean of three separate determinations. Data were fitted to either one or two site Michaelis-Menten inhibition equations (see Methods).

chosen because they contain high proportions of epibatidine binding sites which are resistant to both cytisine and α-CtxMII (Whiteaker *et al*., 2000b). As shown in Figure 1, [^{125}I]-epibatidine bound with high affinity to membranes from the three brain regions investigated. Non-specific binding was less than 2% of specific binding at the highest ligand concentrations used. Specific binding was saturable, and was well described by a single site Hill fit (see Figure 1). In addition, Scatchard analysis (Figure 1, inset) did not suggest systematic deviation from a single site fit. The amount of specific binding observed varied widely among regions, and is summarized in Table 1, together with the calculated K_D and Hill coefficients of binding in each of the regions. The affinity of specific [^{125}I]-epibatidine binding (measured by the K_D values) and Hill coefficients varied very little across regions.

Saturation binding of [^{125}I]-epibatidine fit a single site model. Additionally, no difference was visible between single and two site fits for epibatidine inhibition of [^{125}I]-epibatidine binding in each region (Figure 2, top row). Cytisine inhibition clearly showed the existence of distinct, sensitive (likely to be of the $\alpha_4\beta_2$ subtype; Marks *et al*., 1998) and resistant subpopulations in each region (Figure 2, top row). The binding constants derived for the two ligands are summarized in Table 2. The proportions of cytisine-sensitive and -resistant [^{125}I]-epibatidine binding varied among regions (from approximately 60% in interpeduncular nucleus to approximately 30% in inferior colliculus), but the calculated K_i values for cytisine's interaction at the two sites were extremely similar in all three regions (Table 2).

Inhibition of specific [^{125}I]-epibatidine binding by other agonist ligands

Parker *et al*. (1998) demonstrated that, in addition to cytisine, a number of other agonist ligands (including A85380 and (−)-nicotine) display wide differences in affinity between heterologously expressed nAChR subtypes. Consequently, the inhibition of [^{125}I]-epibatidine binding by A85380 and (−)-nicotine was measured in inferior colliculus, interpeduncular nucleus, and olfactory bulb preparations as shown in Figure 2, bottom row. A population resistant to inhibition by each of the drugs was observed in all three of the regions investigated, and corresponded closely in size to the cytisine-resistant populations in each region (see Table 2). Each drug displayed a different ratio of affinities between its sensitive and resistant sites, but for each compound the ratio of affinities was similar between brain regions. Assuming that the two sites are the same across regions, the average K_i values were: A85380 $=0.031\pm0.005$ nM (sensitive), 31.8 ± 4.5 nM (resistant), ratio = 1026; cytisine = 0.40 ± 0.09 nM (sensitive), 67.4 ± 4.4 nM (resistant), ratio = 169; (−)-nicotine = 3.48 ± 0.30 nM (sensitive), 173 ± 37 nM (resistant), ratio = 50.

Affinities of [^{125}I]-epibatidine at A85380-sensitive and -resistant populations

The results displayed in Figure 2 strongly suggest that each drug (with the exception of epibatidine) differentiated between the same two nAChR populations, which are expressed in varying proportions in inferior colliculus, interpeduncular nucleus and olfactory bulbs. Each drug displayed a different degree of discrimination. The exceptional discrimination displayed by A85380 made it the tool of choice to measure the sizes and affinities of the two [^{125}I]-epibatidine binding populations.

The sizes of the A85380-sensitive and -resistant [^{125}I]-epibatidine binding sites were assessed in each region at differing [^{125}I]-epibatidine concentrations (an example experiment using interpeduncular nucleus membranes is illustrated in Figure 3, top panel). By graphing the sizes of each population at each labelled ligand concentration, saturation curves could be assembled for the A85380-sensitive and -resistant sites (example in Figure 3, bottom panel; see Methods for details). The proportions of sensitive and resistant sites uncovered using this technique varied among brain regions (Table 3), and were very close to those measured by simple inhibition of 200 pM [^{125}I]-epibatidine (see Table 2). As predicted by the experiments illustrated in Figure 1, the affinity of [^{125}I]-epibatidine for both populations was similar, with the A85380-resistant population displaying approximately 2 fold lower affinity for the ligand, when compared to the sensitive population. The Hill coefficient of binding at both sites was approximately 1 in all three regions. These data are summarized in Table 3. Interestingly, both this and the earlier, simpler saturation experiments summarized in Table 1 indicated slightly lower K_D values for [^{125}I]-epibatidine binding to the interpeduncular nucleus, when compared to the other two regions.

A85380-resistant [^{125}I]-epibatidine binding site pharmacology

The initial inhibition binding results (Figure 2) suggested that A85380-resistant binding sites represent a single, distinct nAChR population in the inferior colliculus, interpeduncular nucleus and olfactory bulbs. Co-incubation with a fixed (10 nM) concentration of A85380 allowed selective inhibition of [^{125}I]-epibatidine (200 pM) binding to the A85380-sensitive

Table 2 Inhibition of [^{125}I]-epibatidine binding in inferior colliculus, interpeduncular nucleus, and olfactory bulbs by cytisine, A85380, epibatidine, and (−)-nicotine

	Inferior colliculus			*Interpeduncular nucleus*			*Olfactory bulbs*		
Drug	K_i (sensitive) (nM)	K_i (resistant) (nM)	*% resistant*	K_i (sensitive) (nM)	K_i (resistant) (nM)	*% resistant*	K_i (sensitive) (nM)	K_i (resistant) (nM)	*% resistant*
Cytisine	0.63 ± 0.30	78.1 ± 3.75	30.0 ± 2.2	0.27 ± 0.05	62.3 ± 5.19	58.6 ± 0.1	0.31 ± 0.01	61.8 ± 1.8	48.7 ± 3.3
A85380	0.040 ± 0.023	42.2 ± 4.9	23.9 ± 0.2	0.020 ± 0.001	23.4 ± 5.75	55.3 ± 2.8	0.032 ± 0.022	29.9 ± 1.4	48.5 ± 10.0
Epibatidine	0.025 ± 0.006	Undetectable	N/A	0.016 ± 0.004	Undetectable	N/A	0.034 ± 0.003	Undetectable	N/A
(−)-Nicotine	3.35 ± 2.13	247 ± 94	25.7 ± 4.1	4.17 ± 0.63	89.8 ± 23.5	53.8 ± 0.9	2.91 ± 0.21	183 ± 28	37.0 ± 7.1

Specific [^{125}I]-epibatidine (200 nM) binding in membranes prepared from inferior colliculus, interpeduncular nucleus, and olfactory bulbs was inhibited using cytisine, A85380, epibatidine and (−)-nicotine. Control binding was defined in the absence of competing drug. Values of IC_{50} were calculated for single and two site Michaelis-Menten inhibition fits for each individual experiment. Values of IC_{50} were then converted into K_i values using the Cheng & Prusoff (1973) relationship, with K_D determined from [^{125}I]-epibatidine saturation binding (Table 3). Each value presented is the mean±s.e.mean of three individual determinations. 'Undetectable' indicates that no resistant population was observed. N/A denotes 'not applicable'.

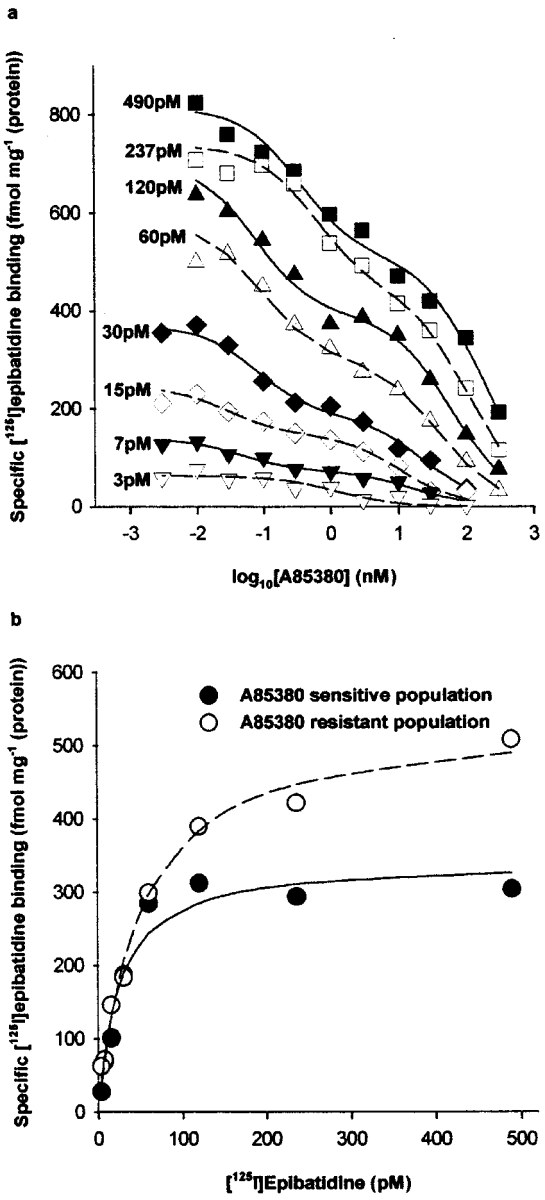

Figure 3 Example experiment: determination of [^{125}I]-epibatidine K_D values at A85380-sensitive and -resistant binding sites in interpeduncular nucleus. (a) Mouse brain interpeduncular nucleus particulate fractions were incubated at 22°C with [^{125}I]-epibatidine (≈4–500 pM; indicated on the left side of each best fit line) in the presence of varying concentrations of A85380 (3 pM–300 nM). Non-specific binding at each [^{125}I]-epibatidine concentration was determined by addition of (−)-nicotine (1 mM), and was subtracted from total binding to determine specific binding at each combination of [^{125}I]-epibatidine and A85380 concentrations. Specific binding was fitted to a two site Michaelis-Menten equation (see Methods), the results of which indicated the densities of the A85380-sensitive and resistant [^{125}I]-epibatidine binding populations at each concentration of labelled ligand. (b) The densities of the A85380-sensitive and resistant [^{125}I]-epibatidine binding populations were plotted at each concentration of labelled ligand, and each population was subjected to Hill saturation analysis, providing values of B_{max}, K_D and n_H for both sites (see Table 3).

population. The pharmacological profiles of the remaining, A85380-resistant binding sites were extensively characterized in each region by inhibition binding experiments, using 19 nicotinic agonists and antagonists. Example inhibition curves are shown in Figure 4, for epibatidine, (−)-nicotine and DHβE in the three regions investigated.

The compounds tested showed widely varying affinities at the A85380-resistant binding sites, as summarized in Table 4. Agonist compounds showed higher affinities (approximately 0.1–5000 nM; epibatidine and acetylcholine respectively) than antagonists (approximately 100–3000 μM; DHβE and hexamethonium respectively). As illustrated in Figure 4, and shown in Table 4, the affinity of each drug was very similar across regions. Importantly, all of the compounds tested inhibited A85380-resistant [^{125}I]-epibatidine binding monophasically, suggesting that A85380-resistant sites represent a single, homogeneous population. Binding was unaffected by the $\alpha_3\beta_2$-selective antagonist α-CtxMII (no effect at concentrations up to 3 μM; see Table 4), confirming earlier work (Whiteaker *et al*., 2000b) that indicated a proportion of [^{3}H]-epibatidine binding in the inferior colliculus, interpeduncular nucleus, and olfactory bulbs is resistant to both cytisine and α-CtxMII.

Autoradiography: distribution of cytisine-resistant [^{3}H]-epibatidine binding, α_3 and β_4 subunit expression

The previous investigation by Whiteaker *et al.* (2000b) suggested that cytisine-resistant [^{3}H]-epibatidine binding sites may be divided into those which are sensitive to α-CtxMII, and a second, more α-CtxMII resistant population, which is the focus of this investigation. As shown in Figure 5, cytisine-resistant epibatidine binding sites in the olfactory bulbs (panel a *vs* panel h), medial habenula–interpeduncular nucleus tract (panels c–e *vs* panels j–l) and the dorsal cortex of the inferior colliculus (panel f *vs* panel m) show little sensitivity to α-CtxMII (20 nM), while those in (for example) the occulomotor nerve and superior colliculus (panel e *vs* panel l) are largely blocked by this moderate α-CtxMII concentration.

Marks *et al.* (1998) suggested that cytisine-resistant epibatidine-binding sites may be associated with α_3 subunits expression, while the generally low agonist affinity of the A85380-resistant [^{125}I]-epibatidine-binding sites was suggestive of a β_4-containing nAChR subtype (Parker *et al*., 1998; Xiao *et al*., 1998). Therefore these sites' distribution was compared to that of α_3 and β_4 mRNA expression, determined by *in situ* hybridization. Expression of α_3 mRNA was restricted to a number of small, well defined nuclei distributed throughout the brain, with the highest densities of expression being found in the olfactory bulbs, medial habenula, substantia nigra, and the superior and inferior colliculi (Figure 5, second to right column). As shown in Figure 5 (right column), the pattern of β_4 mRNA expression in mouse brain is also highly restricted, and is strongly reminiscent of that of the epibatidine-binding sites resistant to both cytisine and α-CtxMII. Very high densities of β_4 mRNA hybridization were observed in the olfactory bulbs, medial habenula, and dorsal cortex of the inferior colliculus. Additional lower densities were seen in a small number of other regions, in particular the interpeduncular nucleus and the cerebellum. As illustrated in Figure 5, the expression patterns of α_3 and β_4 mRNAs do not always overlap (for example see panel r *vs* panel y). However, [^{3}H]-epibatidine binding resistant to both α-CtxMII and cytisine is only found in regions where α_3 and β_4 mRNAs are both expressed, or in regions innervated by those that express both subunits.

Discussion

A previous study from this laboratory (Whiteaker *et al*., 2000b) identified a population of cytisine- and α-CtxMII-resistant [^{3}H]-epibatidine binding nAChRs, primarily located in the inferior colliculus, medial habenula–interpeduncular

Table 3 [^{125}I]-epibatidine saturation binding to A85380-sensitive and -resistant sites in inferior colliculus, interpeduncular nucleus, and olfactory bulbs

	Inferior colliculus			*Interpeduncular nucleus*			*Olfactory bulbs*		
	K_D (pM)	B_{max} (fmol mg^{-1} (protein))	n_H	K_D (pM)	B_{max} (fmol mg^{-1} (protein))	n_H	K_D (pM)	B_{max} (fmol mg^{-1} (protein))	n_H
A85380 sensitive	61.9±17.2	76.5±2.8	1.05±0.04	34.3±8.1	337.5±15.9	1.24±0.14	83.6±30.8	20.0±1.2	1.11±0.05
A85380 resistant	141±53	41.0±1.2	0.95±0.09	64.8±0.8	547±29	0.92±0.07	131±23	19.8±0.6	0.89±0.03

Specific binding of [^{125}I]-epibatidine was determined for differing concentrations in the presence of a range of A85380 concentrations, as described in the Methods section, and demonstrated in Figure 3. Values of B_{max} and K_D were calculated for A85380-sensitive and -resistant binding in each region using the Hill equation. Each value presented is the mean±s.e.mean of three individual determinations.

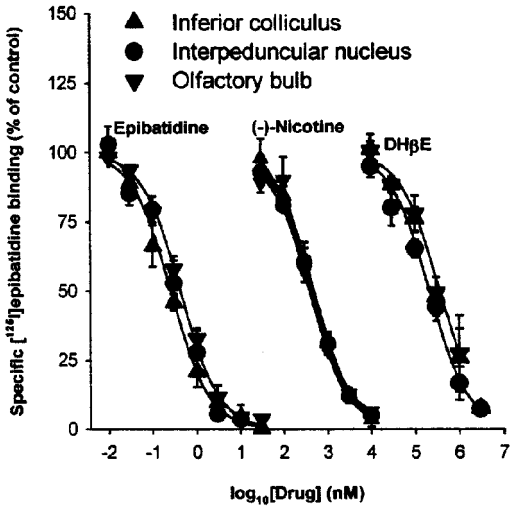

Figure 4 Inhibition of [^{125}I]-epibatidine binding in regionally dissected mouse brain membranes by epibatidine, (−)-nicotine, and DHβE. Particulate fractions prepared from mouse brain inferior colliculus, interpeduncular nucleus, and olfactory bulbs were incubated at 22°C with [^{125}I]-epibatidine (200 pM, 2 h) in the presence of A85380 (10 nM), to selectively block binding to cytisine- (and thus A85380-sensitive) sites. The abilities of drugs (including epibatidine, (−)-nicotine, and DHβE; illustrated) to compete for the remaining, A85380-resistant [^{125}I]-epibatidine binding sites were assessed by including varying concentrations of the test drugs in the incubation. Data from individual experiments were fitted to one site Hill inhibition equations (see Methods). Each point represents the mean±s.e.mean of three separate determinations.

nucleus tract and olfactory bulbs. The combination of [^{3}H]-epibatidine's low specific activity (30–50 Ci mmol^{-1}) and the relative scarcity of the nAChR population of interest precluded the use of this ligand to further probe these receptor's properties. In this study we used the higher specific activity ligand [^{125}I]-epibatidine to perform an extensive pharmacological characterization of these receptors. These sites represent a single pharmacological population, with a distribution and ligand binding properties different from previously characterized central nAChRs.

The high specific activity of [^{125}I]-epibatidine potentially makes it an extraordinarily useful ligand for investigating the properties of scarce nAChR subtypes. The present study confirms this promise: similar to [^{3}H]-epibatidine, [^{125}I]-epibatidine exhibits exceptionally low non-specific binding and high affinity, making possible a detailed pharmacological characterization of a novel neuronal nAChR subtype. [^{125}I]-Epibatidine's slightly lower overall affinity in mouse brain homogenates, when compared to [^{3}H]-epibatidine (K_D = 50–90 and 15–21 pM (Marks *et al*., 1998), respectively) presumably reflected the effect of substituting an ^{125}I for a chlorine atom in the parent compound's chloropyridyl moiety. This result is in agreement with the findings of Badio & Daly (1994), who reported a modest loss of affinity in iodo- *vs* unmodified epibatidine when competing at rat brain (−)-[^{3}H]-nicotine binding nAChRs, and Davila-Garcia *et al*. (1997), who also noted slightly lower affinity of [^{125}I]-epibatidine *vs* [^{3}H]-epibatidine. The slight reduction in affinity associated with iodination may prove helpful in some circumstances, ameliorating ligand depletion problems.

It is highly likely that [^{125}I]-epibatidine and [^{3}H]-epibatidine bind to the same receptor populations in inferior colliculus, interpeduncular nucleus, and olfactory bulbs. Saturation binding analysis demonstrated that the two ligands bind to similar sized populations in the regions of interest. Values of B_{max} determined using [^{125}I]-epibatidine in mouse brain regional homogenates (103.6±2.7 fmol mg^{-1} (protein), 687.3±86.7 fmol mg^{-1} (protein), 29.9±8.5 fmol mg^{-1} (protein) respectively) were similar to the corresponding values reported by Marks *et al*. (1998) using [^{3}H]-epibatidine (93.0±1.5 fmol mg^{-1} (protein), 592.1±7.1 fmol mg^{-1} (protein), 27.7±1.1 fmol mg^{-1} (protein)). Cytisine inhibited [^{125}I]-epibatidine (200 pM) binding to regional homogenates in a biphasic manner. Cytisine-sensitive epibatidine binding corresponds to high affinity nicotine and cytisine binding ($\alpha_4\beta_2$ subtype) nAChRs (Perry & Kellar, 1995; Picciotto *et al*., 1995; Marks *et al*., 1998; Marubio *et al*., 1999). The proportions of cytisine-resistant [^{125}I]-epibatidine binding sites (30.0±2.2, 58.6±0.1, and 48.7±3.3% in inferior colliculus, interpeduncular nucleus, and olfactory bulbs respectively) observed were again similar to those reported in the same regions using [^{3}H]-epibatidine (500 pM) by Marks *et al*. (1998) (33.6, 62.6, and 56.2%). Together, the saturation and cytisine inhibition binding data strongly indicate that [^{125}I]-epibatidine and [^{3}H]-epibatidine label the same nAChR populations in the regions of interest. Because the proportion of cytisine-resistant binding sites varies among regions, it is likely these sites represent a population or populations distinct from the already characterized cytisine sensitive, $\alpha_4\beta_2$ nAChRs.

In addition to cytisine, [^{125}I]-epibatidine (200 pM) binding to regional homogenates was inhibited by A85380, epibatidine and (−)-nicotine. If [^{125}I]-epibatidine binds to the different nAChRs with a similar ratio of affinities to the native compound, one would expect to see monophasic displacement of the labelled compound by its unlabelled counterpart. As shown in Figure 2, this was indeed the case. Inhibition by A85380 and (−)-nicotine provided initial evidence that the same populations of nAChRs are expressed (in different proportions) across the three brain regions. Both A85380 and (−)-nicotine produced biphasic inhibition of [^{125}I]-epibatidine binding in each of the regions tested. Within each region, a similar proportion of binding was resistant to each of the competing ligands. In addition, each drug exhibited similar affinities at sensitive and resistant sites across regions.

Table 4 Inhibition of A85380-resistant [^{125}I]-epibatidine binding in inferior colliculus, interpeduncular nucleus, and olfactory bulbs

Compound	*Inferior colliculus* K_i (nM)	*Interpeduncular nucleus* K_i (nM)	*Olfactory bulb* K_i (nM)	*Average* (K_i) *across regions* K_i (nM)
Agonists				
Acetylcholine	2345±1462	5313±619	5886±1192	4515±1097
Anabasine	6101±3140	4601±2201	2233±438	4312±1126
Anatoxin-a	26.3±14.8	6.28±2.44	11.1±3.8	14.6±6.0
Cytisine	121±13	66±15	263±125	150±59
DMPP	1143±262	406±53	1394±681	981±296
(±)-Epibatidine	0.10±0.03	0.10±0.04	0.16±0.01	0.12±0.02
Epiboxidine	3.24±0.87	0.92±0.36	5.94±2.72	3.37±1.45
Lobeline	4141±615	2604±124	6761±3694	4502±1214
MCC	697±129	489±21	928±101	705±127
(−)-Nicotine	208±44	114±23	179±30	167±28
(+)-Nicotine	2676±752	1228±276	1784±378	1896±422
Nornicotine	4649±3355	1602±533	1891±325	2714±971
TMA	777±259	268±29	469±53	505±148
UB-165	4.44±1.00	1.90±0.10	4.79±1.51	3.71±0.91
Antagonists				
α-CtxMII	No effect	No effect	No effect	No effect
Decamethonium	$2.89\pm0.55\times10^6$	$1.70\pm0.33\times10^6$	$2.06\pm0.37\times10^6$	$2.22\pm0.35\times10^6$
DHβE	146677±57762	98168±26856	198175±28461	147673±28874
Hexamethonium	$2.87\pm1.02\times10^6$	$2.18\pm0.29\times10^6$	$2.99\pm0.20\times10^6$	$2.68\pm0.25\times10^6$
d-Tubocurarine	103161±26263	59463±15982	52992±3584	71872±15756

The abilities of nicotinic compounds to inhibit A85380 (10 nM)-resistant [^{125}I]-epibatidine (200 pM) binding were determined in binding experiments, as illustrated in Figure 4. Values of IC_{50} were calculated for each individual experiment using the Hill inhibition equation, and then converted into K_i values using the Cheng & Prusoff (1973) relationship, with K_d as determined for the A85380-resistant portion of binding in each brain region (Table 3). Each value presented is the mean±s.e.mean of three individual determinations.

The high affinity and exceptional selectivity of A85380 for (−)-[^{3}H]-nicotine binding sites has been established by previous workers (Abreo *et al*., 1996; Mukhin *et al*., 2000), and facilitated the measurement of [^{125}I]-epibatidine affinity at both the agonist-sensitive and -resistant sites (Figure 3). The small affinity differences detected for [^{125}I]-epibatidine binding to cytisine-sensitive ($\alpha_4\beta_2$) and -resistant sites in this study (Table 3), when compared to those seen using [^{3}H]-epibatidine (Houghtling *et al*., 1995; Flores *et al*., 1996) are similar to the findings of Davila-Garcia *et al*. (1997), and suggest that iodination reduces the affinity of epibatidine binding more at $\alpha_4\beta_2$ than some other nAChR subtypes.

A85380 was used to pharmacologically isolate the A85380- (and hence cytisine-) resistant sites for further investigation. As illustrated in Figure 4 and Table 4, the K_i values of the drugs tested at the A85380-resistant site are very similar across regions. In addition, none of the drugs' inhibition of A85380-resistant [^{125}I]-epibatidine binding showed any detectable deviation from a single site fit. Together, these data strongly suggest that A85380-resistant sites in the inferior colliculus, interpeduncular nucleus, and olfactory bulbs represent a single nAChR population. Although these sites are expressed in isolated brain nuclei, they comprise a large proportion of the nAChR population in the regions where they are located. This fact, together with electrophysiological data suggesting a functional role for a non-$\alpha_4\beta_2$ nAChR subtype in the habenulo-interpeduncular tract (Mulle *et al*., 1991; Zoli *et al*., 1998) suggests that they may have a significant physiological role in the mammalian CNS.

The evidence gathered in this study is insufficient to positively identify the specific subtype of the A85380-resistant [^{125}I]-epibatidine-binding population. However, the data provide circumstantial evidence that the sites may be of the $\alpha_3\beta_4$ subtype. First, the pharmacological profile of A85380-resistant [^{125}I]-epibatidine-binding sites closely matches that ascribed to heterologously expressed $\alpha_3\beta_4$ nAChRs, as described by Parker *et al*. (1998), and Xiao *et al*. (1998). Further, Mukhin *et al*. (2000) showed the exquisite selectivity of A85380 binding to mouse and rat brain $\alpha_4\beta_2$-subtype nAChRs, and derived an 800 fold affinity difference for A85380 between rat brain $\alpha_4\beta_2$-subtype nAChRs and $\alpha_3\beta_4$-subtype nAChRs expressed in rat adrenal gland, very similar to that reported between agonist-sensitive and -resistant sites in the present study. Second, A85380-resistant [^{125}I]-epibatidine-binding sites are found in regions which express both α_3 and β_4 mRNA (such as the olfactory bulbs, accessory olfactory bulbs, medial habenula, dorsal cortex of the inferior colliculus, and the prepositus hypoglossal and medial vesibular nuclei), or are innervated by those that do (the interpeduncular nucleus, which receives considerable cholinergic innervation from the medial habenula *via* the fasciculus retroflexus; Clarke *et al*., 1986). Third, Zoli *et al*. (1998) report that high affinity [^{3}H]-epibatidine-binding sites with low affinities for both [^{3}H]-cytisine and (−)-[^{3}H]-nicotine ('type 3' receptors) persist in the interpeduncular nucleus and inferior colliculus of β_2-null mutant mice (these authors did not examine olfactory bulbs), demonstrating independence of β_2 subunit expression. These authors also recorded electrophysiological responses in the habenulo-interpeduncular tracts of β_2-null mutant mice, with an activation pharmacology suggestive of $\alpha_3\beta_4$ subtype nAChRs. Similarly, high affinity [^{3}H]-epibatidine binding persists in the interpeduncular nucleus and medial habenula of α_4-null mutant mice (Marubio *et al*., 1999).

It is important to remember that although suggestive, these lines of evidence do not prove that the A85380-resistant [^{125}I]-epibatidine-binding population is of the $\alpha_3\beta_4$ subtype. For instance, other subunits may be included in the putatively α_3 and β_4 receptor complex, with subtle effects on binding pharmacology (such as β_3 or α_6; see Groot-Kormelink *et al*., 1998 and Fucile *et al*., 1998, respectively). Alternatively, it is possible that other, uncharacterized subunit combinations may produce a similar pharmacology. Thus, definitive assignation of a particular nAChR subunit combination to this novel subtype will require further experimentation. Possible approaches would include immunoisolation with subunit-specific antibodies (as performed by Flores *et al*. (1996) for trigeminal

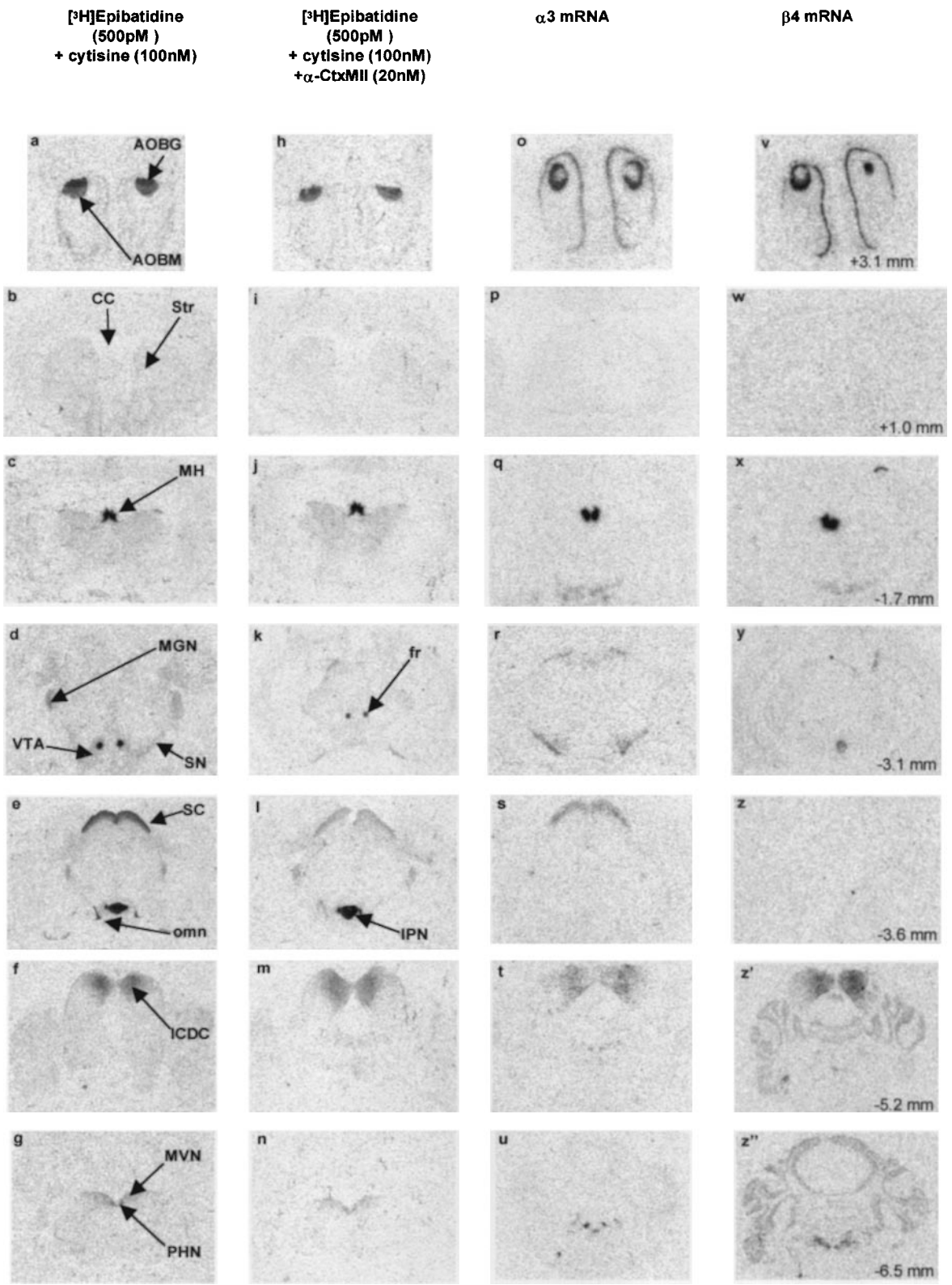

Figure 5 Autoradiographic comparison of [^{3}H]-epibatidine (500 pM) binding in the presence of cytisine (100 nM; cytisine-resistant binding) with that in the presence of cytisine + α-CtxMII (100 and 20 nM, respectively; cytisine- and α-CtxMII-resistant binding), and α_3 and β_4 mRNA expression in mouse brain. Sections (14 μm) were incubated in the presence of 500 pM [^{3}H]-epibatidine + 100 nM cytisine (left column), 500 pM [^{3}H]-epibatidine + 100 nM cytisine + 20 nM α-CtxMII (second-to-left column), or were subjected to α_3 or β_4 mRNA *in situ* hybridization (α_3 mRNA second-to-right column; β_4 mRNA right-hand column) as described in the Methods section. Panels are digital images of autoradiograms, approximate distances relative to the bregma are shown in the right column. Abbreviations for the indicated brain regions are: AOBG, accessory olfactory bulb glomerular layer; AOBM, accessory olfactory bulb mitral layer; CC, corpus callosum; fr, fasciculus retroflexus; ICDC, inferior colliculus, dorsal cortex; IPN, interpeduncular nucleus; MGN, medial geniculate nucleus; MH, medial habenula; MVN, medial vestibular nucleus; omn, occulomotor nerve; PHN, prepositus hypoglossal nucleus; SC, superior colliculus; SN, substantia nigra; Str, striatum; VTA, ventral tegmental area.

ganglion nAChRs), or use of subunit-null mutant animals (such as reported by Zoli *et al*., 1998; Whiteaker *et al*., 2000a). Fortunately, it seems likely that the distinctive pharmacology of this novel site will facilitate such efforts.

The results in this study indicate the presence of a novel central nervous system nAChR population, located primarily in the inferior colliculus, interpeduncular nucleus, and olfactory bulbs. These sites represent a single pharmacological class of nicotinic binding sites, displaying pharmacology and distribution incompatible with previously characterized nicotinic populations. This study also demonstrates that [^{125}I]-epibatidine may be used, in conjunction with selective pharmacology, to identify and characterize novel and scarce native nAChR subtypes. Given the high affinity of epibatidine for a multitude of nAChR subtypes (Parker *et al*., 1998), this general approach is likely to be widely applicable.

This work was supported by grants DA-12242, DA-03194 and DA-10156 from the National Institute on Drug Abuse, and NIH grants MH-53631 and GM-48677. A.C. Collins is supported, in part, by Research Scientist Award DA-00197 from the National Institute on Drug Abuse.

References

ABREO, M.A., LIN, N.-H., GARVEY, D.S., GUNN, D.E., HETTINGER, A.-M., WASICAK, J.T., PAVLIK, P.A., MARTIN, Y.C., DONNELLY-ROBERTS, Y.C., ANDERSON, D.J., SULLIVAN, J.P., WILLIAMS, M., ARNERIC, S.P. & HOLLADAY, M.W. (1996). Novel 3-pyridyl ethers with subnanomolar affinity for central neuronal nicotinic acetylcholine receptors. *J. Med. Chem.,* **39,** 817–825.

BADIO, B. & DALY, J.W. (1994). Epibatidine: a potent analgetic and nicotinic agonist. *Mol. Pharmacol.,* **45,** 563–569.

CARTIER, G.E., YOSHIKAMI, D., GRAY, W.R., LUO, S., OLIVERA, B.M. & MCINTOSH, J.M. (1996). A new α-conotoxin which targets $\alpha_3\beta_2$ nicotinic acetylcholine receptors. *J. Biol. Chem.,* **271,** 7522–7528.

CHENG, Y.-C. & PRUSOFF, W.H. (1973). Relationship between the inhibition constant (K_i) and the concentration of inhibitor which causes 50 per cent inhibition (I_{50}) of an enzymatic reaction. *Biochem. Pharmacol.,* **22,** 3099–3108.

CLARKE, P.B.S., HAMILL, G.S., NADI, N.S., JACOBOWITZ, D.M. & PERT, A. (1986). ^{3}H Nicotine-labeled and ^{125}I α-Bungarotoxin-labeled nicotinic receptors in the interpeduncular nucleus of rats. 2. Effects of habenular deafferentation. *J. Compar. Neurol.,* **251,** 407–413.

COX, K.H., DELEON, L.M., ANGERER, L.M. & ANGERER, R.C. (1984). Detection of mRNAs in sea urchin embryos by *in situ* hybridization using asymmetric RNA probes. *Dev. Biol.,* **101,** 485–502.

DANI, J.A. & HEINEMANN, S. (1996). Molecular and cellular aspects of nicotine abuse. *Neuron,* **16,** 905–908.

DAVILA-GARCIA, M.I., MUSACHIO, L.J., PERRY, D.C., XIAO, Y., HORTI, A., LONDON, E.D., DANNALS, R.F. & KELLAR, K.J. (1997). [^{125}I]IPH, an epibatidine analog, binds with high affinity to neuronal nicotinic cholinergic receptors. *J. Pharmacol. Exp. Ther.,* **282,** 445–451.

DECKER, M.W. & ARNERIC, S.P. (1998). Nicotinic acetylcholine receptor-targeted compounds: a summary of the developmental pipeline and therapeutic potential. In *Neuronal Nicotinic Receptors, Pharmacology and Therapeutic Opportunities.* ed Americ S.P. & Brioni J.D., pp. 395–411. New York: Wiley Liss.

FLORES, C.M., DECAMP, R.D., KILO, S., ROGERS, S.W. & HARGREAVES, K.M. (1996). Neuronal nicotinic receptor expression in sensory neurons of the rat trigeminal ganglion: demonstration of $\alpha_3\beta_4$, a novel subtype in the mammalian nervous system. *J. Neurosci.,* **16,** 7894–7901.

FLORES, C.M., ROGERS, S.W., PABREZA, L.A., WOLFE, B.B. & KELLAR, K.J. (1992). A subtype of nicotinic cholinergic receptor in the brain is composed of α_4 and β_2 subunits and is upregulated by chronic nicotine treatment. *Mol. Pharmacol.,* **41,** 31–37.

FUCILE, S., MATTER, J.-M., ERKMAN, L., RAGOZZINO, D., BARABINO, B., GRAZZI, F., ALEMÀ, S., BALLIVET, M. & EUSEBI, F. (1998). The neuronal alpha6 subunit forms heteromeric acetylcholine receptors in human transfected cells. *Eur. J. Neurosci.,* **10,** 172–178.

GROOT-KORMELINK, P.J., LUYTEN, W.H., COLQUHOUN, D. & SIVILOTTI, L.G. (1998). A reporter mutation approach shows incorporation of the "orphan" subunit beta3 into a functional nicotinic receptor. *J. Biol. Chem.,* **273,** 15317–15320.

HOUGHTLING, R.A., DAVILA-GARCIA, M.I., HURT, S.D. & KELLAR, K.J. (1995). Characterization of [^{3}H]epibatidine binding to nicotinic receptors in rat and human brain. *Mol. Pharmacol.,* **48,** 280–287.

LINDSTROM, J., ANAND, R., GERZANICH, V., PENG, X., WANG, F. & WELLS, G. (1996). Structure and function of neuronal nicotinic acetylcholine receptors. *Prog. Brain Res.,* **109,** 125–137.

LOWRY, A., ROSEBROUGH, N.J., FARR, A.L. & RANDALL, R.J. (1951). Protein measurement with the Folin phenol reagent. *J. Biol. Chem.,* **193,** 263–275.

MARKS, M.J., PAULY, J.R., GROSS, S.D., DENERIS, E.S., HERMANS-BORGMEYER, I., HEINEMANN, S.F. & COLLINS, A.C. (1992). Nicotine binding and nicotinic receptor subunit mRNA after chronic nicotine treatment. *J. Neurosci.,* **12,** 2765–2784.

MARKS, M.J., SMITH, K.W. & COLLINS, A.C. (1998). Differential agonist inhibition identifies multiple epibatidine binding sites in mouse brain. *J. Pharmacol. Exp. Ther.,* **285,** 377–386.

MARUBIO, L.M., ARROYO-JIMENEZ, M.M., CORDERO-ERAUSQUIN, M., LÉNA, C., LENOVÈRE, N., EXAERDE, A.K., HUCHET, M., DAMAJ, M.I. & CHANGEUX, J.-P. (1999). Reduced antinociception in mice lacking neuronal nicotinic receptor subunits. *Nature,* **398,** 805–810.

MUKHIN, A.G., GÜNDISCH, D., HORTI, A.G., KOREN, A.O., TAMAGNAN, G., KIMES, A.S., CHAMBERS, J., VAUPEL, D.B., KING, S.L., PICCIOTTO, M.R., INNIS, R.B. & LONDON, E.D. (2000). 5-Iodo-A-85380, an $\alpha_4\beta_2$ subtype-selective ligand for nicotinic acetylcholine receptors. *Mol. Pharmacol.,* **57,** 642–649.

MULLE, C., VIDAL, C., BENOIT, P. & CHANGEUX, J.P. (1991). Existence of different subtypes of nicotinic acetylcholine receptors in the rat habenulo-interpeduncular system. *J. Neurosci.,* **11,** 2588–2597.

ORR-URTREGER, A., GOLDNER, F.M., SAEKI, M., LORENZO, I., GOLDBERG, L., DEBIASI, M., DANI, J.A., PATRICK, J.W. & BEAUDET, A.L. (1997). Mice deficient in the alpha 7 neuronal nicotinic acetylcholine receptor lack alpha-bungarotoxin binding sites and hippocampal fast nicotinic currents. *J. Neurosci.,* **17,** 9165–9171.

PARKER, M.J., BECK, A. & LUETJE, C.W. (1998). Neuronal nicotinic receptor β_2 and β_4 subunits confer large differences in agonist binding affinity. *Mol. Pharmacol.,* **54,** 1132–1139.

PAULY, J.R., STITZEL, J.A., MARKS, M.J. & COLLINS, A.C. (1989). An autoradiographic analysis of cholinergenic receptors in mouse brain. *Brain Res. Bull.,* **22,** 453–459.

PERRY, D.C. & KELLAR, K.J. (1995). [^{3}H]Epibatidine labels nicotinic receptors in rat brain: an autoradiographic study. *J. Pharmacol. Exp. Ther.,* **275,** 1030–1034.

PICCIOTTO, M.R., ZOLI, M., LENA, C., BESSIS, A., LALLEMAND, Y., LENOVERE, N., VINCENT, P., MERLO-PICH, E., BRULET, P. & CHANGEUX, J.-P. (1995). Abnormal avoidance learning in mice lacking functional high-affinity nicotine receptor in mouse brain. *Nature (Lond.),* **274,** 65–67.

SCHOEPFER, R., CONROY, W.G., WHITING, P., GORE, M. & LINDSTROM, J. (1990). Brain α-bungarotoxin binding protein cDNAs and mAbs reveal subtypes of this branch of the ligand-gated ion channel gene superfamily. *Neuron,* **5,** 35–48.

SEGUELA, P., WADICHE, J., DINELEY-MILLER, K., DANI, J.A. & PATRICK, J.W. (1992). Molecular cloning, functional properties and distribution of rat brain α_7: a nicotinic cation channel highly permeable to calcium. *J. Neurosci.,* **13,** 596–604.

SIMMONS, D.M., ARRIZA, J.L. & SWANSON, L.W. (1989). A complete protocol for *in situ* hybridization of messenger RNAs in brain and other tissues with radiolabeled single-stranded RNA probes. *J. Histotechnol,* **12,** 169–181.

WHITEAKER, P., MARKS, M.J., GRADY, S.R., LU, Y., PICCIOTTO, M.R., CHANGEUX, J.-P. & COLLINS, A.C. (2000a). Pharmacological and null mutation approaches reveal nicotinic receptor diversity. *Eu. J. Pharmacol.,* **393,** 123–135.

WHITEAKER, P., MCINTOSH, J.M., LUO, S., COLLINS, A.C. & MARKS, M.J. (2000b). ^{125}I-α-Conotoxin MII identifies a novel nicotinic acetylcholine receptor population in mouse brain. *Mol. Pharmacol.,* **57,** 913–925.

WHITING, P. & LINDSTROM, J. (1987). Purification and characterization of nicotinic acetylcholine receptor from rat brain. *Proc. Natl. Acad. Sci. U.S.A.,* **84,** 595–599.

XIAO, Y., MEYER, E.L., THOMPSON, J.M., SURIN, A., WROBELOWSKI, J. & KELLAR, K.J. (1998). Rat $\alpha_3\beta_4$ subtype of neuronal nicotinic acetylcholine receptor stably expressed in a transfected cell line: pharmacology of ligand binding and function. *Mol. Pharmacol.,* **54,** 322–333.

ZOLI, M., LÉNA, C., PICCIOTTO, M.R. & CHANGEUX, J.-P. (1998). Identification of four classes of brain nicotinic receptors using β_2 mutant mice. *J. Neurosci.,* **18,** 4461–4472.

(Received April 28, 2000
Revised July 13, 2000
Accepted July 21, 2000)